M2+(Ni, Cu, Zn)Al-LDH Composites with Hydrochar from Rambutan Peel and Study the Adsorption Efficiency for Organic Dyes.pdf

By Risfidian Mohadi

M^{2+}(Ni, Cu, Zn)/Al-LDH Composites with Hydrochar from Rambutan Peel and Study the Adsorption Efficiency for Organic Dyes

Risfidian Mohadi[1], Normah[2], Neza Rahayu Palapa[3], and Aldes Lesbani[1,3*]

[1]*Graduate School of Faculty Mathematics and Natural Sciences, Sriwijaya University, Palembang-South Sumatera, Indonesia*
[2]*Magister Programme Graduate School of Mathematics and Natural Sciences, Sriwijaya University, Palembang-South Sumatera, Indonesia*
[3]*Research Center of Inorganic Materials and Coordination Complexes, Faculty of Mathematics and Natural Sciences, Sriwijaya University, Palembang-South Sumatera, Indonesia*

ARTICLE INFO

Received: 5 Nov 2021
Received in revised: 26 Dec 2021
Accepted: 9 Jan 2022
Published online: 1 Feb 2022
DOI: 10.32526/ennrj/20/202100218

Keywords:
LDH-Hc composite/ Rambutan peel/ Selectivity/ Recyclable/ Adsorption

*** Corresponding author:**
E-mail: aldeslesbani@pps.unsri.ac.id

ABSTRACT

Ni/Al LDH, Cu/Al LDH, and Zn/Al LDH were composed with rambutan peel hydrochar (Hc) and the materials were applied as adsorbent for the removal of methylene blue from aqueous solution, measured using UV-Vis Spectrophotometric method. The preparation of the LDH-Hc composites were proven by XRD, FT-IR, and SEM analysis which showed similar characteristics of the LDH-Hc composites with pure LDH and hydrochar. The methylene blue removal efficiency was optimized by various parameters including adsorption selectivity, adsorption regeneration, pH, contact time, adsorption concentration, and temperature. The adsorption study analysis proved that LDH composited with rambutan peel hydrochar had a selective ability for methylene blue. Zn/Al-hydrochar had the most stable adsorption regeneration ability and adsorbed MB easily after seven regeneration cycles using water solvents and ultrasonic devices. Ni/Al-hydrochar and Cu/Al-hydrochar were effective up to five regeneration cycles for MB removal. The adsorption results showed that the optimal pH for MB adsorption was at pH 6 with an equilibrium adsorption contact time of 100 min and a tendency to follow the pseudo second order kinetic model. Parameter data of concentration and temperature of adsorption was determined using Langmuir and Freundlich equations. The results showed that the adsorption matched the Freundlich isotherm model with the adsorption capacity (q_m) of Ni/Al-Hc, Cu/Al-Hc, and Zn/Al-Hc adsorbents reaching 144.928, 175.439, 217.391 mg/g, respectively, with the adsorption process taking place continuously, spontaneously, and endothermically.

1. INTRODUCTION

Methylene blue (MB) is the most widely used dye in industry (Xu et al., 2020) such as pharmaceutical, paper, textile, paint, and plastic industries (Ahmad et al., 2020; Dang et al., 2020; Mantasha et al., 2020; Wang et al., 2016). Dyestuff waste is one of the environmental pollution problems that must be overcome to ensure sustainable industrial production (Nakhli et al., 2020). Methylene blue is a cationic dye that is classified as a toxic dye with mutagenic and carcinogenic properties that will significantly affect human health which can cause neuronal apoptosis, increased heart rate, inflammation of the leptomeninges, nausea, and vomiting and harm aquatic ecosystems (Alver et al., 2020; Liao et al., 2020; Nakhli et al., 2020).

Therefore, industrial waste treatment needs to be carried out to reduce the concentration of waste before being discharged into the environment. To overcome pollution in wastewater, various methods can be used such as adsorption, photocatalytic separation (Karagöz et al., 2008), membrane processes, coagulation, biodegradation (Li et al., 2020a), flocculation (Li et al., 2020b), aerobic and anaerobic treatment, ion exchange and electrochemistry (Ebadollahzadeh and Zabihi, 2020). Among them, the simplest, cheapest, and most effective wastewater treatment process is adsorption

Citation: Mohadi R, Normah, Palapa NR, Lesbani A. M^{2+}(Ni, Cu, Zn)/Al-LDH composites with hydrochar from rambutan peel and study the adsorption efficiency for organic dyes. Environ. Nat. Resour. J. 2022;20(2):221-233. (https://doi.org/10.32526/ennrj/20/202100218)

(Badri et al., 2020), one of the main industrial wastewater treatment methods for effluent purification. Adsorption is a method of transferring pollutant molecules to solid materials that can selectively remove pollutants from liquid waste by attracting pollutant molecules to the surface of the adsorbent (Alver et al., 2020). However, to reduce processing costs, efforts can be made to use alternative adsorbents that are cheap, abundant and easy to find. Recently, many studies have developed inexpensive and effective adsorbents to remove dyes in industrial waste made from agricultural wastes (Alinezhad et al., 2020). In the literature, a number of adsorbents have been investigated such as clay (Adeyemo et al., 2017), duku peel (Juleanti et al., 2021), wood waste (Stjepanović et al., 2021), orange peel (Chopra et al., 2012), plant biomass (Yeow et al., 2021), pineapple (Mahmuda et al., 2021), rice husk (Palapa et al., 2020a), coconut husk, bamboo dust (Rafatullah et al., 2010), and rambutan peel (Normah et al., 2021a).

Rambutan peel has been reported to have main chemical components containing cellulose, lignin, hemicellulose and phenolic compounds. This research conducted by Castro and das Virgens (2019) supports the effective application of rambutan skin as an adsorbent. Some of the advantages of rambutan peel as an adsorbent include having a good adsorption capacity, selective adsorption and can be regenerated (Mahmuda et al., 2021; Alrozi et al., 2012; Setiawan et al., 2018). Therefore, the conversion of rambutan peel into an adsorbent will provide an alternative that has the potential to be modified with layered double hydroxide to form a composite.

Layered double hydroxide or LDH is an anionic clay material that has a two-dimensional (2D) structure and contains anions in the interlayer, LDH is the same as hydrotalcite which is composed of divalent (M^{2+}) and trivalent (M^{3+}) metals which have the general formula $[M^{2+}_{1-x}M^{3+}_{x}(OH)_2] [A^{n-}_{x/n}]\cdot mH_2O$, A^{n-}: interlayer anions as charge balance (Lu et al., 2020; Xu et al., 2021). LDH has the advantage of producing a material that has a large adsorption capacity and is flexible (Lesbani et al., 2020; Normah et al., 2021b). However, LDH cannot be recycled and cannot be used in a regeneration process. Therefore, a method is needed to produce a stronger structure so that it can be used repeatedly by being composited with a supporting material (Wijaya et al., 2021).

Based on several investigations, LDH can be composited with biochar, zeolite, graphite, and chitosan (Bezerra et al., 2021; Fang et al., 2021). Zubair et al. (2018) reported that Ni/Fe LDH was composited with starch and applied to remove methyl orange in the liquid phase with a maximum adsorption capacity of 387.59 mg/g and a stable regeneration cycle reaching four cycles for the starch composite adsorbent NiFe-LDH. Alagha et al. (2020) reported Mg-Fe/LDH magnetic composite with activated carbon was applied to remove nitrate and phosphate in wastewater with reusability performance results with five regeneration cycles.

This study aimed to modify the LDH in the form of Ni/Al, Cu/Al, and Zn/Al composites with hydrochar rambutan peel, characterized using XRD, FT-IR, and SEM analysis. The adsorbent was applied for the selectivity of organic dyes in the form of methylene blue (MB), Rhodamine-B (Rh-B), methyl orange (MO), methyl red (MR), then the adsorbent would be tested for effectiveness in studies of regeneration, adsorption isotherms, and adsorption thermodynamics with the most selective dyes with adsorbents.

2. METHODOLOGY

2.1 Materials

The chemicals used to synthesize materials are nickel(II) nitrate ($Ni(NO_3)_2\cdot 3H_2O$, 99% purity) by Sigma Aldrich, copper(II) nitrate ($Cu(NO_3)_2\cdot 3H_2O$, 98% purity) by LOBA Chemie, zinc(II) nitrate ($Zn(NO_3)_2\cdot 3H_2O$, 98.9% purity) by Merck, aluminum(III) nitrate, ($Al(NO_3)_3.9H_2O$, MW=375.13 g/mol, 98% purity) by Sigma Aldrich, hydrochloric acid (HCl, MW=36.458 g/mol, 37%), sodium hydroxide (NaOH, MW=40.00 g/mol by Merck, and the basic ingredient for making hydrochar is rambutan peel. Adsorbate used dye methylene blue (MB), Rhodamine-B (Rh-B), methyl orange (MO), and methyl red (MR).

2.2 Methods

2.2.1 Rambutan peel preparation

Rambutan peel powder was prepared using rambutan peel that had been cleaned and then dried in the sun. The dried rambutan peel was cut into small pieces and then baked at 110°C for 8 h. Then, the peel was mashed and passed through a 50 mesh sieve.

2.2.2 Hydrochar (Hc) preparation

Hydrochar was prepared using the hydrothermal carbonization (HTC) method (Li et al., 2020c) using a stainless steel autoclave hydrothermal device with 2.5 g of rambutan peel powder and 50 mL of distilled water tightly closed in the oven at 200°C for 10 h. In the final process, the autoclave was cooled to room temperature and the product in the autoclave was filtered. The resulting solid (hydrochar) was dried at a temperature of 105°C. Hydrochar was analyzed by characterization with XRD, FT-IR, and SEM.

2.2.3 Composite LDH-Hc preparation

The preparation of LDHs into LDH-Hc composites was carried out by the coprecipitation method by preparing 30 mL of a solution of M^{2+} (Ni, Cu, and Zn) (0.75 M) mixed with 30 mL (0.25 M) aluminum (III) nitrate and stirred. A 2 M NaOH solution was added dropwise to the mixture until it reached pH 10 and was maintained for 1 h until a precipitate was formed. To the LDH-Hc composite precipitate mixture was added as much as 3 g of hydrochar powder from rambutan peel, then stirred and kept at 80°C for 72 h. The product from the process was filtered using a vacuum and rinsed with distilled water, and the resulting product was then dried at 60°C to dryness. The preparation results in the form of Ni/Al-Hc, Cu/Al-Hc, and Zn/Al-Hc were analyzed by XRD, FT-IR, and SEM.

2.2.4 Adsorption experiment procedure

Adsorption selectivity is done by mixing several dyes using the same concentration and the same volume of dye. The dyes were methylene blue (MB), rhodamine-B (Rh-B), methyl orange (MO), and methyl red (MR) with a concentration of 8 mg/L each of 50 mL, then the mixture was added to 0.05 g (rambutan peel, Hc, Ni/Al-Hc, Cu/Al-Hc, and Zn/Al-Hc) and stirred using a shaker with time variations of 0, 15, 30, 60, to 120 min. After the expiration of each time, the mixture is separated by centrifugation to obtain the filtrate and residue. The filtrate is then analyzed for wavelength using a UV-Vis spectrophotometer in the range of 400-700 nm.

After obtaining the most selective dye, methylene blue (MB), adsorption studies using MB were done on each adsorbent.

The adsorption process of MB was studied through the influence of adsorption time. Various of the adsorption times were carried out with the concentration of MB 60 mg/L, then 20 mL was taken and added as much as 0.02 g of adsorbent and stirred for 0-150 min.

The kinetics adsorption was calculated using kinetic adsorption model such as pseudo first-order (PFO) and pseudo second-order (PSO). The formula should be written by:

$$\text{Pseudo first-order (PFO): } \log\left(q_e - q_t\right) = \log q_e - \left(\frac{k_1}{2{,}303}\right) t \quad (1)$$

$$\text{Pseudo first-order (PFO): } \frac{t}{q_t} = \frac{1}{k2\,qe^2} + \frac{1}{q_e} t \quad (2)$$

Where; q_e is adsorption capacity at equilibrium (mg/g); q_t is adsorption capacity at t (mg/g); t is adsorption time (min); k_1 is adsorption kinetic rate at pseudo first-order (/min); k_2 is adsorption kinetic rate at pseudo second-order (g/mg/min).

The adsorption isotherm model in the form of Langmuir and Freundlich models was used to determine the equilibrium adsorption capacity data and analyze the adsorption mechanism.

Langmuir and Freundlich isotherm equations are as follows:

$$\text{Langmuir: } \frac{C}{m} = \frac{1}{bK} + \frac{C}{b}\frac{C}{m} = \frac{1}{bK_{ML}} + \frac{C}{b} \quad (3)$$

Where; C is a saturated concentration of adsorbate; m is the amount of adsorbate; b is the maximum adsorption capacity (mg/g); K_{ML} is the Langmuir constant (mg/L).

$$\text{Freundlich: } \text{Log}\, q_e = \log K_F + \frac{1}{n}\log C \quad (4)$$

Where; q_e is adsorption capacity at equilibrium (mg/g); C_e is a concentration of adsorbate at equilibrium (mg/L); K_F is Freundlich constant.

The experimental adsorption isotherm was carried out with various initial concentrations of methylene blue (MB) (60, 70, 80, 90, and 100 mg/L) As much as 20 mL of MB solution was added to 0.02 g of adsorbent (rambutan peel, Hc, Ni/Al-Hc, Cu/Al-Hc and Zn/Al-Hc) and stirred for 2 h with temperature variations of 30, 40, 50, and 60°C. The last process was the separation of solutions and solids using centrifugation, then the solution was measured using a UV-Vis Spectrophotometer.

Adsorption thermodynamics used to calculate the Gibbs free energy change data (ΔG), enthalpy (ΔH), and entropy (ΔS) calculated by Equation (5-6):

$$\Delta G = -RT \ln (K_d) \quad (5)$$

$$\ln K_d = \frac{\Delta S}{R} - \frac{\Delta H}{RT} \quad (6)$$

K_d is the solute distribution coefficient (L/g); R is the universal gas constant (8.314 mol/K); T is temperature (K); Gibbs free energy (ΔG, kJ/mol); entropy (ΔS, kJ/mol); and enthalpy (ΔH, J/mol/K).

The regeneration process was carried out to test the effectiveness of the adsorbent in reusing the adsorbent. In this study, the regeneration process was carried out by adding 50 mL of adsorbate solution and 0.5 g of adsorbent (rambutan peel, Hc, Ni/Al-Hc, Cu/Al-Hc, and Zn/Al-Hc). The mixture of adsorbent and adsorbate was stirred for 3 h then separated between the solution and residual adsorbent, the solution was taken and measured using a UV-Vis spectrophotometer, while the remaining adsorbent was dried at 40°C and reused through the desorption process. The desorption process was carried out by adding 50 mL of water to the residual adsorbent and then desorption using an ultrasonic device for 2 h. The adsorbent that has gone through the desorption process is dried and then reused for the next adsorption process for seven repetitions of the same procedure.

3. RESULTS AND DISCUSSION

The successful preparation of LDH-Hc composite materials in the form of Ni/Al-Hc, Cu/Al-Hc, and Zn/Al-Hc was proven by the results of XRD, FT-IR, and SEM characterization analysis. The data characterization results are shown in Figure 1. Figure 1(a) shows an XRD diffractogram of rambutan peel with the appearance of two distinctive peaks at diffraction angles of 16° and 23.3° which describe that the rambutan peel contains cellulose compounds (Oliveira et al., 2016). Figure 1(b) shows the diffractogram of Hc material from the preparation of rambutan peel through the hydrothermal carbonization (HTC) process and shows a diffraction pattern similar to Figure 1(a). In the Hc diffractogram there was an increase in crystallinity, this was due to changes in amorphous cellulose compounds. The results of XRD characterization of composite materials were confirmed through the JCPDS (Joint Committee on Powder Diffraction Standard) data corresponding to each LDH. Typical diffraction peaks of Ni/Al LDH according to JCPDS data No.15-0087 (Wang et al., 2018), Cu/Al LDH with JCPDS No. 30-0630 (Palapa et al., 2020b) and Zn/Al LDH with JCPDS No. 48.2023 (Shin et al., 2020). The diffraction patterns of the Mg/Al-Hc, Ca/Al-Hc, and Zn/Al-Hc composites are presented in Figure 1.

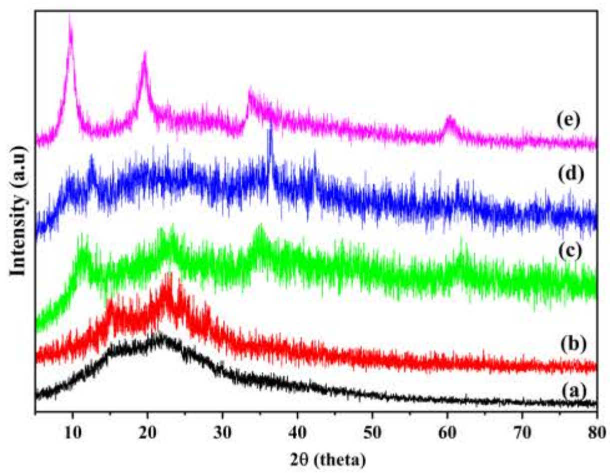

Figure 1. X-ray Powder diffraction patterns of rambutan peel (a), Hc (b), Ni/Al-Hc (c), Cu/Al-Hc (d), and Zn/Al-Hc (e)

Based on Figure 1, the diffraction peaks in Figure 1(c) which show the Ni/Al-Hc diffractogram at 2 θ angles 11.38°(003), 22.9°(002), 35.2°(012), 61.6°(110). The peaks that emerge are described as typical peaks of the layered structure. The diffraction peaks of Ni/Al-Hc composite materials were in accordance with JCPDS No. 15-0087 with diffraction of 2θ 10.9°(003), 34.5°(012), and 61.6°(110). The diffraction peaks of the Cu/Al-Hc composite material shown in Figure 1(d) have diffraction peaks at 12.75°(003), 18.9°(002), 36.44°(012), and 61.5°(110) was identified as a layered structure according to JCPDS No.30-0630. Figure 1(e) shows the Zn/Al-Hc difactogram with peaks at 2 θ angles around 9.78°(003), 19.66°(002), 33.80°(012), and 60.24°(110) according to JCPDS No. 48.2023. In addition, Figure 1 shows a typical diffraction peak of Hc around 19° to 22.9° with a reflection plane (002) identified as a cellulose compound from rambutan peel. Based on the results of the analysis, the preparation of composite materials in the form of Ni/Al-Hc, Cu/Al-Hc, and Zn/Al-Hc has been successfully prepared as evidenced by the appearance of diffraction peaks for pure LDH and Hc as the base material.

The successful preparation of the LDH-Hc composite material is supported by the FT-IR characterization presented in Figure 2. The spectra of the Ni/Al-Hc, Cu/Al-Hc, and Zn/Al-Hc composites have the characteristics of pure LDH and Hc, which appear about 3,424 cm^{-1} which corresponds to the vibration of the -OH group on the surface of the LDH layer, the peak of 1,635 cm^{-1} indicates the vibration of water molecules between the LDH layer, the vibration at the peak of about <1,000 cm^{-1} indicates the presence of metal molecules bound to oxygen in the LDH layer. LDHs (M-O, M-O-M, O-M-O) are characteristics of LDH (Hu et al., 2019). In addition, the vibrations that appear in 2953 cm^{-1} are associated with the C-H group, the 1,683 cm^{-1} peak associated with the C-O group and the 1,013 cm^{-1} peak associated with the C=C group which is characteristic of cellulose compounds in Hc materials (Castro and das Virgens, 2019). The LDH-Hc composite material has a vibration similar to that of pure LDH and Hc. FT-IR data confirm the successful modification of LDH with Hc.

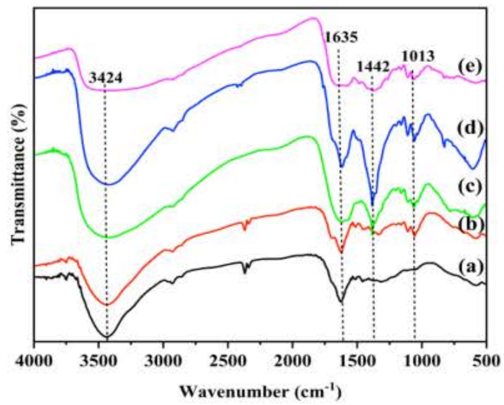

Figure 2. Spectrum FT-IR of Rambutan peel (a), Hc (b), Ni/Al-Hc (c), Cu/Al-Hc (d), and Zn/Al-Hc (e)

SEM analysis is used to see the surface morphology of the material. The results of the SEM analysis of the material are presented in Figure 3. The rambutan peel shown in Figure 3(a) has a surface morphology with flat-shaped particles but heterogeneous in size and rough surface texture, while the Hc shown in Figure 3(b) has a surface morphology with particles shaped like round like a ball and more homogeneous in size. This is caused by the degradation of lignin and cellulose compounds in rambutan peels during the carbonization process. LDH-Hc in the form of Ni/Al-Hc (c), Cu/Al-Hc (d) and Zn/Al-Hc (e) has a rough, uneven surface texture and irregular pores and has a pore size of large pores with high aggregates.

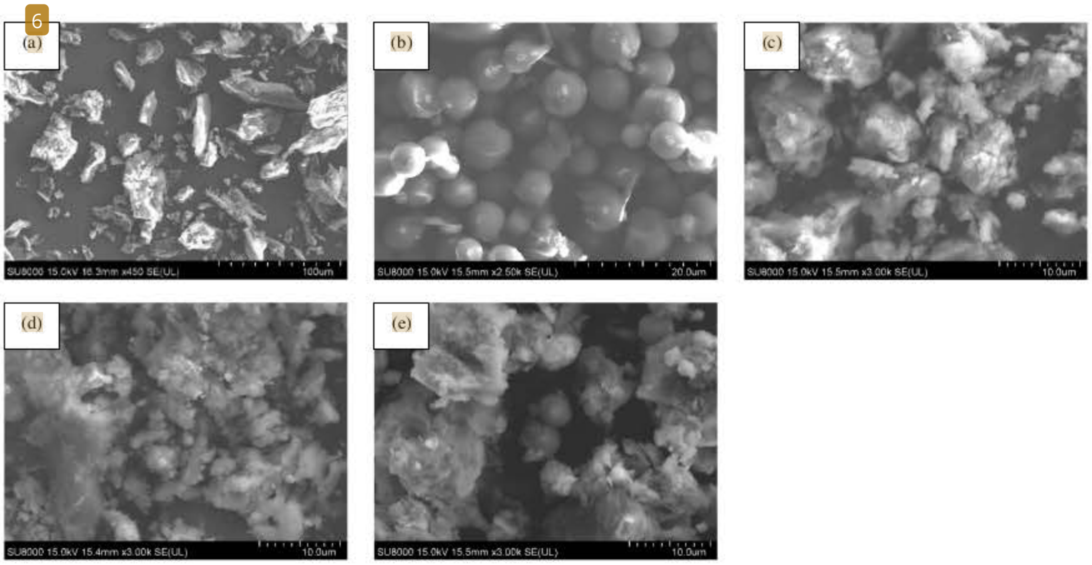

Figure 3. SEM image of Rambutan peel (a), Hc (b), Ni/Al-Hc (c), Cu/Al-Hc (d), and Zn/Al-Hc (e)

The adsorption selectivity was carried out by mixing four dyes in the form of methylene blue (MB), rhodamine-B (Rh-B), methyl red (MR), and methyl orange (MO) with a concentration of 8 mg/L added to each of the peel adsorbents. rambutan, Hc, Ni/Al-Hc, Cu/Al-Hc, and Zn/Al-Hc, and the wavelength at the maximum absorbance of the mixed dye solution was measured using a UV-Vis spectrophotometer. The results of these measurements are presented in Figure 4. The adsorption selectivity of the mixed dye was analyzed from changes in the adsorbed concentration which progressively increased during the adsorption process from 0, 15, 30, 60, to 120 min. Figure 4 shows the results of the adsorption selectivity on MB dye at first 8.33 mg/g, rambutan peel to 4.11 mg/g, Hc to 2.56 mg/g, Ni/Al-Hc to 0.2 mg/g, Cu/Al-Hc to 1.68 mg/g, and Zn/Al-Hc to 0.26 mg/g. Rh-B dye was initially 8.26 mg/g, rambutan peel was 6.01 mg/g, Hc to 2.45 mg/g, Ni/Al-Hc to 1.04 mg/g, Cu/Al-Hc to 3.98 mg/g, Zn/Al-Hc to 0.71 mg/g, for MR dyes initially at first of 8.13 mg/g, rambutan peel of 6.01 mg/g, Hc to 6.53 mg/g, Ni/Al-Hc to 2.64 mg/g, Cu/Al-Hc to 5.13 mg/g, and Zn/Al-Hc to 2.8 mg/g. MO at first was 8.24 mg/g, rambutan peel was 8.18 mg/g, Hc to 5.87 mg/g, Ni/Al-Hc to 3.49 mg/g, Cu/Al-Hc to 4.12 mg/g, and Zn/Al-Hc to 3.83 mg/g. A drastic decrease occurred at minute 120 with each adsorbent adsorbent. It can be concluded that the dye is selective for the adsorbent of rambutan peel, Hc, Ni/Al-Hc, Cu/Al-Hc, and Zn/Al-Hc are MB dye. After knowing

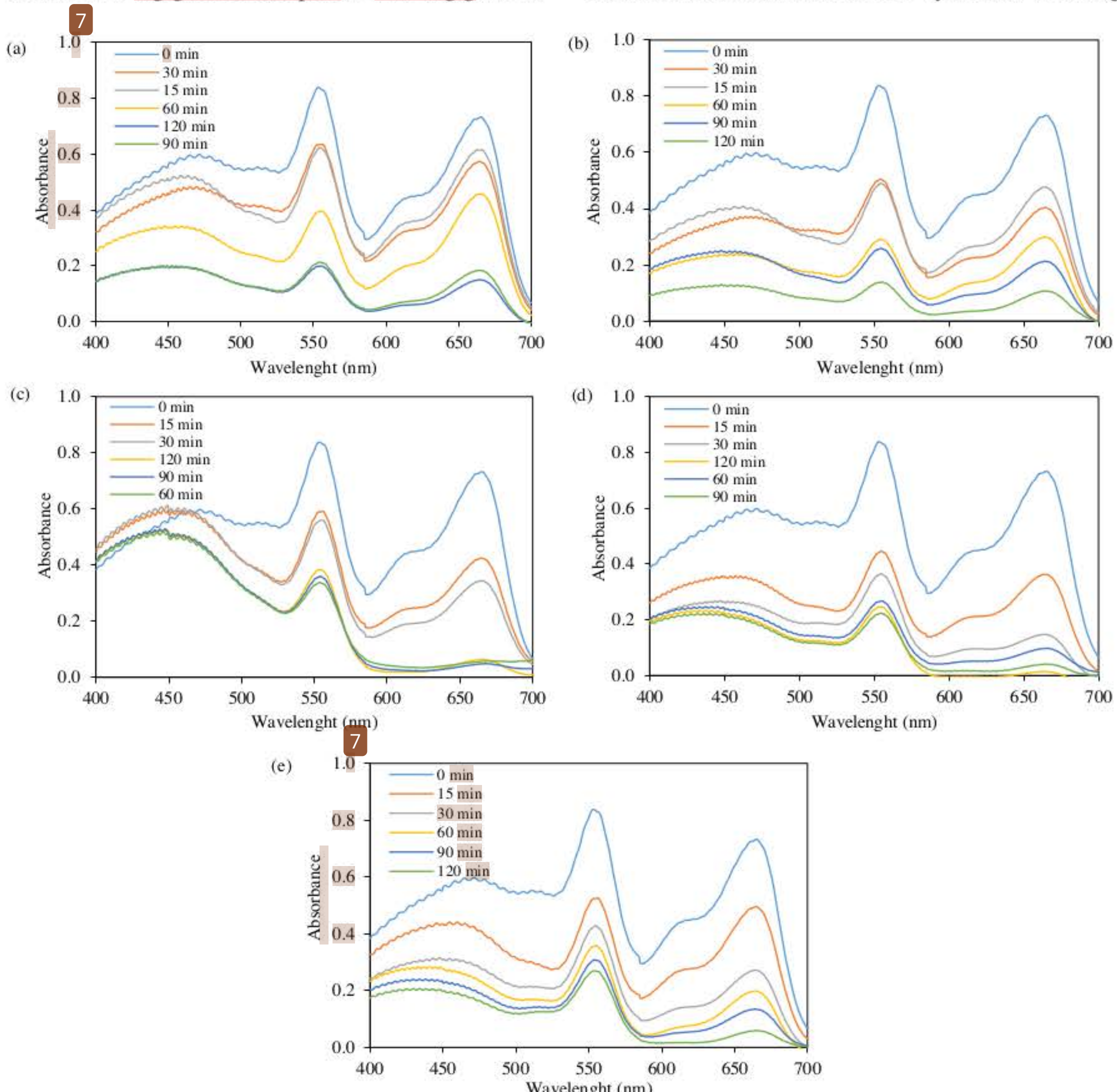

Figure 4. UV-Visible spectra of mixture MB, Rh-B, MR, and MO on Rambutan peel (a), Hc (b), Ni/Al-Hc (c), Cu/Al-Hc (d), and Zn/Al-Hc (e)

the most selective dye was MB, then MB was continued for the adsorption process using regeneration studies and adsorption isotherms and thermodynamic adsorption processes to determine the effectiveness of the adsorbent in removing MB.

Furthermore, conducting a regeneration study to determine the effectiveness of each adsorbent for repeated use. The results of the study regeneration of rambutan peel, Hc, Ni/Al-Hc, Cu/Al-Hc, and Zn/Al-Hc are shown in Figure 5.

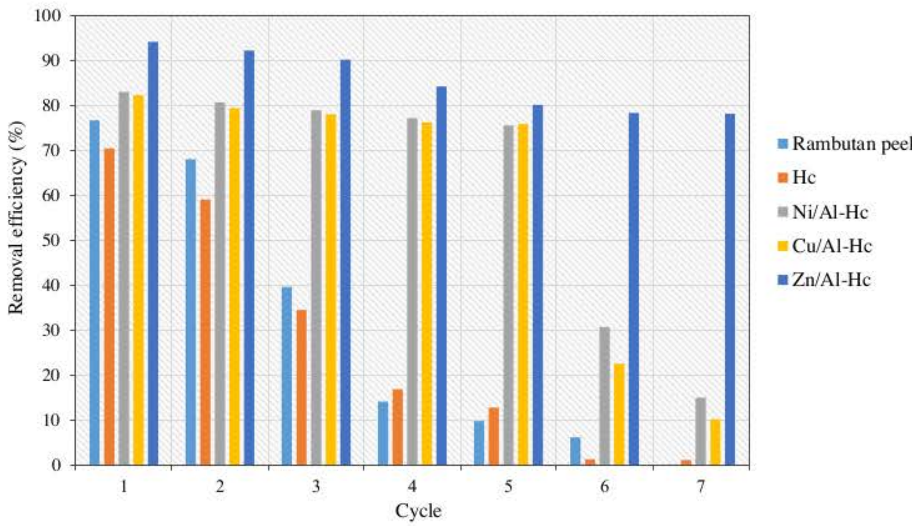

Figure 5. Rambutan peel, Hc, Ni/Al-Hc, Cu/Al-Hc, and Zn/Al-Hc adsorbent regeneration ability

Rambutan peel, Hc, Ni/Al-Hc, and Cu/Al-Hc composites showed a decrease in adsorption ability. Rambutan peel had an adsorption capacity of 76.65% in the first cycle and decreased to 0.12% in the last cycle. Hc has a cycle I of 70.43%, and its ability also decreased to 1.09% in the last cycle. The results of the regeneration of Zn/Al-Hc composites showed a stable adsorption ability compared to Ni/Al-Hc and Cu/Al-Hc. Ni/Al-Hc reached 83.02% in the first cycle and decreased to 14.98% for the last cycle, while Cu/Al-Hc in the first cycle was 82.29% and the last cycle decreased to 10.13%. Zn/Al-Hc reached the first cycle of 94.13%, the second was 92.19%, the third was 90.13%, the fourth was 84.21%, the fifth was 80.12%, the sixth was 78.33% and the last one was 78.11%. Rambutan peel, Hc, Ni/Al-Hc, and Cu/Al-Hc experienced a very significant decrease while the Zn/Al-Hc composite material decreased but not significantly. Based on these data, Zn/Al-Hc has the best regeneration ability compared to rambutan peel, Hc, Ni/Al-Hc, and Cu/Al-Hc.

The variation of pH adsorption of methylene blue using rambutan peel adsorbents, Hc, Ni/Al-Hc, and Cu/Al-Hc is shown in Figure 6.

On rambutan peel Hc, Ni/Al-Hc, Cu/Al-Hc, and Zn/Al-Hc the maximum adsorption of MB occurred at the optimum pH which was pH 6. Experiments with pH variations were generally carried out to determine the optimum pH for MB adsorption. Based on Mantasha et al. (2020), the OH^- ion from the adsorbent at acidic pH of blue will maintain the N group in the methylene dye, so that the interaction between methylene blue and the adsorbent will increase and the attractive force that occurs is also getting bigger. Meanwhile, at alkaline pH, methylene blue forms a salt that ionizes the negatively charged Cl^- group and at the same time OH^- ions from the adsorbent will inhibit the absorption process caused by the formation of repulsion by the same charge around the surface of the adsorbent with a charge of methylene blue dye. Which causes the methylene blue dye to be difficult to apply to the adsorbent surface.

The adsorption ability on the adsorption kinetics parameters can be seen in Figure 7. Find the adsorption kinetics model using Equations 1 and 2 in the form of Pseudo First Order (PFO) and Pseudo Second Order (PSO) equations. Adsorbents Hc, Ni/Al-Hc, Cu/Al-Hc and Zn/Al-Hc composites on the MB adsorption kinetics process showed that the absorption time occurred at 100 min. The parameters calculated from Equations 1 and 2 are shown in Table 1.

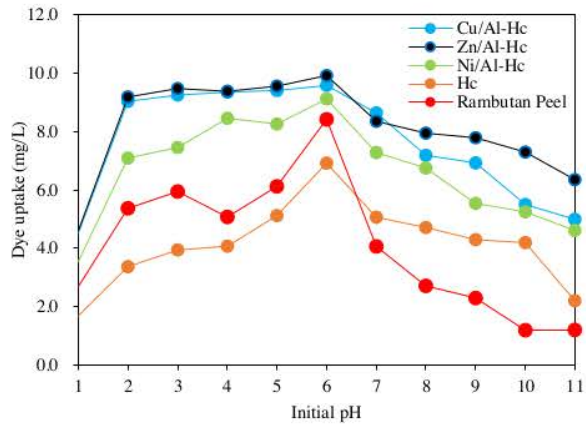

Figure 6. The effect of pH on adsorption capacity of adsorbent (rambutan peel, Hc, Ni/Al-Hc, Cu/Al-Hc, Zn/Al-Hc) and removal of MB

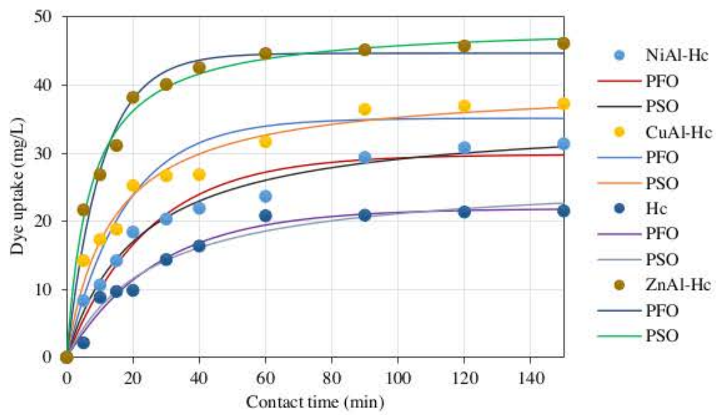

Figure 7. Adsorption kinetics model of MB using Hc, Ni/Al-Hc, Cu/Al-Hc, and Zn/Al-Hc

Table 1. Kinetic parameters of dyes adsorption onto Hc, Zn/Al-Hc, Cu/Al-Hc, and Ni/Al-Hc

Adsorbent	$Qe_{experiment}$ (mg/g)	PFO			PSO		
		Qe_{Calc} (mg/g)	R^2	k_1	Qe_{Calc} (mg/g)	R^2	k_2
Hc	46.143	24.400	0.938	0.037	47.619	0.998	0.097
Zn/Al-Hc	44.705	41.763	0.974	0.038	49.261	0.995	0.007
Cu/Al-Hc	31.381	29.356	0.970	0.030	35.971	0.993	0.022
Ni/Al-Hc	21.450	24.160	0.965	0.047	27.173	0.952	0.016

One of the most important characteristics in the adsorption process is kinetics. To clarify the adsorption kinetics of MB using the Hc, Ni/Al-Hc, Cu/Al-Hc, and Zn/Al-Hc composites adsorbent, the kinetic models, PFO and PSO were used. For the study of adsorption kinetics, the concentration of MB used was 50 mg/L with varying times ranging from 0 to 180 min and 0.02 g of adsorbent was added at the optimum condition of pH 6. The PSO model as the equation was assumed to be ideal on the adsorption surface of MB. The constant values of K1 and q_e were calculated from the slope and intercept log (q_e-q_t) versus t (Equations 1-2).

Table 1 shows that the adsorption kinetics tend to follow the PSO model with a linear regression value that is closer to 1 (R^2>0.952). Each adsorbent reached the optimal q_e value with the adsorption equilibrium time at 100 minutes. The largest value of q_e It can be seen that the PSO model is almost right for the first step. However, the PSO kinetic model seen from the highest linear regression R^2 (Table 1) and seen from the adsorption capacity value calculated from the pseudo model is close to the experimental value, which shows that the dominant kinetic phenomenon of PSO for MB adsorption by the adsorbent Hc, Ni/Al-Hc, Cu/Al-Hc, and Zn/Al-Hc composites with the dominant adsorption process occurring chemical interactions between the adsorbent and the adsorbate.

Furthermore, the adsorption ability is determined through the isotherm parameters which can be presented in Figure 8. Determination of the adsorption isotherm is determined through the Langmuir and Freundlich equations based on Equations 3 and 4.

Figure 8 shows the Langmuir and Freundlich isotherm model pattern. Figure 8 shows that the Zn/Al-Hc composite material has a higher adsorbed concentration (q_e) than rambutan peel, Hc, Ni/Al-Hc, and Cu/Al-Hc. Figure 6 on rambutan peel, Hc, Ni/Al-Hc, Cu/Al-Hc looks lower for MB adsorption. Determination of the adsorption isotherm model through the linear regression value of R^2 which is close to 1. The calculated data are presented in Table 2.

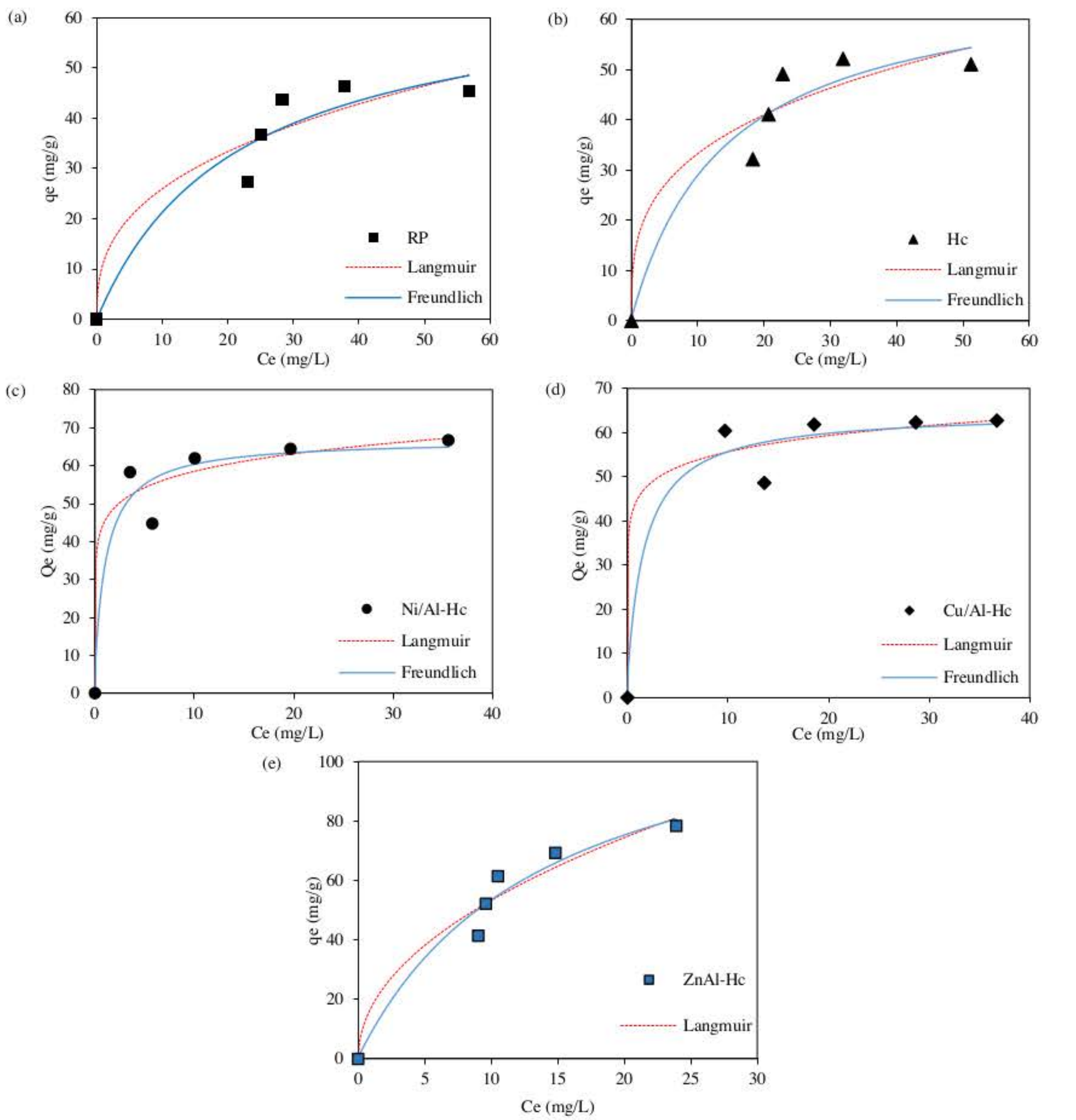

Figure 8. Adsorption isotherm model of MB using Rambutan peel (a), Hc (b), Ni/Al-Hc (c), Cu/Al-Hc (d), and Zn/Al-Hc (e)

Table 2 shows the Langmuir and Freundlich isotherm data in the form of Langmuir constant (kL), maximum adsorption capacity (q_m), adsorption intensity (n), and Freundlich constant (kF). Table 1 shows the Langmuir data at the Langmuir constant value (kL) of 0.070, 0.080, 0.025, 0.074, 0.040 and is in the range of 0 and 1 which identifies a suitable system for the adsorption process (Mishra et al., 2020; Zhao et al., 2020). The q_m data shows the value of large adsorption capacity on the adsorbent of LDH-Hc composite materials (Ni/Al-Hc, Cu/Al-Hc, Zn/Al-Hc) reaching 144.928 mg/g, 175.439 mg/g, 217.910 mg/g while rambutan peel precursors and Hc had lower adsorption capacities of 43.860 mg/g and 49.286 mg/g, respectively. Furthermore, Table 2 is equipped with data on the Freundlich isotherm with the value of the Freundlich constant (kF) and the value of n where the kF value reaches 0.921 to 20.029 which is related to the binding energy between the adsorbate and the adsorbent, while the adsorption intensity (n) with a value of n reaches 0.285 to 10.560 related according to the adsorption process.

Based on Table 2, the adsorption process tends to follow the Freundlich isotherm according to the linear coefficient value (R^2) which is closer to 1. Freundlich isotherm is an adsorption process following adsorption by multilayer adsorption and Freundlich can also describe physical adsorption (Wang et al., 2020) is supported by a value of $1/n<1$ (Table 2) as the intensity of multilayer adsorption of adsorbate molecules on the surface of a heterogeneous material (Binh and Nguyen, 2020).

Table 2. Isotherm model of MB adsorption on Rambutan peel, Hc, Ni/Al-Hc, Cu/Al-Hc, and Zn/Al-Hc

Materials	Langmuir			Freundlich		
	q_m (mg/g)	kL	R^2	n	kF	R^2
Rambutan peel	43.860	0.070	0.995	0.285	20.029	0.999
Hc	49.286	0.080	0.999	4.651	4.870	0.999
Ni/Al-Hc	144.928	0.025	0.991	2.699	10.737	0.999
Cu/Al-Hc	175.439	0.074	0.936	10.560	0.921	0.999
Zn/Al-Hc	217.391	0.040	0.989	1.863	15.153	0.994

The comparison of MB adsorption for several adsorbents is presented in Table 3. Table 3 shows the adsorption capacity of several adsorbents for MB dye. Comparison between the performance of the adsorbent and various adsorbents that have a value (q_m) which is associated with the maximum adsorption capacity of the adsorbent for the removal of the adsorbent in the form of MB. It can be seen that Ni/Al-Hc, Cu/Al-Hc, and Zn/Al-Hc have a larger adsorption capacity in MB removal, this is due to the large surface area and more active sites of LDH and Hc. so that the interaction of the adsorbate with the adsorbent is more so that the adsorption capacity is large. The adsorbents prepared in this study have higher adsorption capacities when compared with the ones on Table 3.

Furthermore, the thermodynamic parameters provide data on the Gibbs free energy (ΔG), enthalpy (ΔH), and entropy (ΔS) which are calculated according to Equations 3 and 4. The adsorption thermodynamic data are shown in Table 4.

Table 4 shows the results of the calculation of negative adsorption values for ΔG on each adsorbent. ΔG values increase with increasing adsorption temperature from 30°C to 60°C. A negative value ΔG indicates that the MB adsorption process takes place spontaneously (Normah et al., 2021b). In this study, the ΔH value showed a range of 10.851 kJ/mol to 42.1[illegible] kJ/mol which was related to the tendency of MB adsorption to occur by physical adsorption and a positive ΔH value indicated that MB adsorption was endothermic (Wijaya et al., 2021). The value of S° is positive and is in the range of 0.037 J/mol·K to 0.144 J/mol·K. This is related to the irregularity of the particles during the adsorption process which increases due to the interaction between solid in the form of adsorbent-liquid in the form of MB adsorbate.

Table 3. Comparison of several adsorbents to removal MB

Adsorbent	Adsorption capacity (mg/g)	Reference
Cellulosic olice stones biomass	22.4	Al-Ghouti and Al-Absi (2020)
Fe_3O_4@C_{60}@MA	7.51	Xu et al. (2020)
Scenedesmus microalgae	55.26	Rathee et al. (2019)

Table 3. Comparison of several adsorbents to removal MB (cont.)

Adsorbent	Adsorption capacity (mg/g)	Reference
Bio-adsorbent of Pleurotus eryngii	18.45	Wu et al. (2019)
PDOPA-f-Mg/Al LDH	132	Zhao et al. (2017)
MnMgFe	20	Khuluk et al. (2019)
Ni/Fe/Ti LDH	29.940	Rathee et al. (2019)
Mg3AlDBS	10.864	Abdellaoui et al. (2019)
Rambutan peel	57.803	In this study
Hc	49.286	In this study
Ni/Al-Hc	144.928	In this study
Cu/Al-Hc	175.439	In this study
Zn/Al-Hc	217.391	In this study

Table 4. Thermodynamic parameters of MB adsorption on Rambutan peel, Hc, Ni/Al-Hc, Cu/Al-Hc, and Zn/Al-Hc

Parameters	T (K)	Materials				
		Rambutan peel	Hc	Ni/Al-Hc	Cu/Al-Hc	Zn/Al-Hc
ΔG	303	-0.210	-0.430	-1.479	-0.368	-1.373
	313	-0.566	-0.956	-2.076	-0.739	-2.809
	323	-1.011	-1.481	-2.672	-1.109	-4.246
	333	-1.807	-2.007	-3.269	-1.479	-5.682
ΔS		0.053	0.053	0.060	0.037	0.144
ΔH		15.503	15.503	16.593	10.851	42.150

4. CONCLUSION

In this study, LDH in the form of Ni/Al, Cu/Al, and Zn/Al were synthesized using the coprecipitation method and modified with hydrochar from rambutan peel which was prepared using the hydrothermal carbonization method. The material was applied as an adsorbent for the removal of methylene blue in aqueous solution using UV-Vis spectrophotometric method. The manufacture of LDH-Hc composites was proven by XRD, FT-IR, and SEM analysis. The results of adsorption selectivity showed that LDH with rambutan peel hydrochar showed good selective ability for methylene blue d and regeneration studies showed that the LDH-Hc composite showed a more stable adsorption regeneration ability reaching seven regeneration cycles for Zn/Al-Hc, while Ni/Al-Hc and Cu/Al-Hc achieved five regeneration cycles compared to LDH without modification, which only achieved three regeneration cycles using water solvent. The optimum pH of MB was found at pH 6. The study of adsorption kinetics was carried out using pseudo first order and pseudo second order equations and the removal of conformity MB followed the pseudo second order kinetic model. Parameter data of concentration and temperature of adsorption using Langmuir and Freundlich equation was determined. The results showed that the adsorption matched the Freundlich isotherm model with adsorption capacity (q_m) using Ni/Al-Hc, Cu/Al-Hc, and Zn/Al-Hc adsorbents reaching 144.928, 175.439, and 217.391 mg/g, respectively, with the adsorption process taking place continuously, spontaneously, and endothermically. The performance of the LDH-Hc composite using the adsorption method is superior to many other materials that have been used for dye absorption in the literature.

ACKNOWLEDGEMENTS

Authors thank Research Center of Inorganic Materials and Complexes, FMIPA Sriwijaya University for support this research.

REFERENCES

Abdellaoui K, Pavlovic I, Barriga C. Nanohybrid layered double hydroxides used to remove several dyes from water. ChemEngineering 2015;3(2):Article No. 41.

Adeyemo AA, Adeoye IO, Bello OS. Adsorption of dyes using different types of clay: A review. Applied Water Science 2017;7(2):543-68.

Ahmad A, Jini D, Aravind M, Parvathiraja C, Ali R, Kiyani MZ, et al. A novel study on synthesis of egg shell based activated carbon for degradation of methylene blue via photocatalysis. Arabian Journal of Chemistry 2020;13(12):8717-22.

Al-Ghouti MA, Al-Absi RS. Mechanistic understanding of the adsorption and thermodynamic aspects of cationic methylene blue dye onto cellulosic olive stones biomass from wastewater. Scientific Reports 2020;10(1):Article No. 15928.

Alagha O, Manzar MS, Zubair M, Anil I, Mu'azu ND, Qureshi A. Magnetic Mg-Fe/LDH intercalated activated carbon composites for nitrate and phosphate removal from wastewater: Insight into behavior and mechanisms. Nanomaterials 2020;10(7):Article No. 1361

Alinezhad H, Zabihi M, Kahfroushan D. Design and fabrication the novel polymeric magnetic boehmite nanocomposite (boehmite@ Fe_3O_4@PLA@SiO_2) for the remarkable competitive adsorption of methylene blue and mercury ions. Journal of Physics and Chemistry of Solids 2020;144:Article No. 109515.

Alrozi R, Zamanhuri NA, Osman MS. Removal of methylene blue from aqueous solution by adsorption onto NaOH-treated rambutan peel. 2012 IEEE Business, Engineering and Industrial Applications Colloquium (BEIAC) 2012;5:92-7.

Alver E, Metin AÜ, Brouers F. Methylene blue adsorption on magnetic alginate/rice husk bio-composite. International Journal of Biological Macromolecules 2020;154:104-13.

Badri A, Alvarez-Serrano I, Luisa López M, Ben Amara M. Sol-gel synthesis, magnetic and methylene blue adsorption properties of lamellar iron monophosphate $KMgFe(PO_4)_2$. Inorganic Chemistry Communications 2020;121:Article No. 108217.

Bezerra BGP, Bieseki L, de Mello MIS, da Silva DR, Rodella CB, Pergher S. Memory effect on a LDH/zeolite a composite: An XRD in situ study. Materials 2021;14(9):Article No. 2102.

Binh QA, Nguyen HH. Investigation the isotherm and kinetics of adsorption mechanism of herbicide 2,4-dichlorophenoxyacetic acid (2,4-D) on corn cob biochar. Bioresource Technology Reports 2020;11:Article No. 100520.

Castro JDS, das Virgens CF. Thermal decomposition of *Nephelium lappaceum* L. peel: Influence of chemical pretreatment and evaluation of pseudo-components by Fraser-Suzuki function. Journal of Thermal Analysis and Calorimetry 2019;138(5):3541-9.

Chopra M, Drivjot, Amita. Adsorption of dyes from aqueous solution using orange peels: Kinetics and equilibrium. Journal of Advanced Laboratory Research in Biology 2012;3(1):1-8.

Dang W, Zhang J, Nie H, Wang F, Tang X, Wu N, et al. Isotherms, thermodynamics and kinetics of methane-shale adsorption pair under supercritical condition: Implications for understanding the nature of shale gas adsorption process. Chemical Engineering Journal 2020;383:Article No. 123191.

Ebadollahzadeh H, Zabihi M. Competitive adsorption of methylene blue and Pb (II) ions on the nano-magnetic activated carbon and alumina. Materials Chemistry and Physics 2020;248:Article No. 122893.

Fang Q, Ye S, Yang H, Yang K, Zhou J, Gao Y, et al. Application of layered double hydroxide-biochar composites in wastewater treatment: Recent trends, modification strategies, and outlook. Journal of Hazardous Materials 2021;420:Article No. 126569.

Hu X, Li P, Zhang X, Yu B, Lv C, Zeng N, et al. Ni-based catalyst derived from NiAl layered double hydroxide for vapor phase catalytic exchange between hydrogen and water. Nanomaterials 2019;9(12):Article No. 1688.

Juleanti N, Palapa NR, Taher T, Hidayati N, Putri BI, Lesbani A. The capability of biochar-based CaAl and MgAl composite materials as adsorbent for removal Cr (VI) in aqueous solution. Science and Technology Indonesia 2021;6(3):156-65.

Karagöz S, Tay T, Ucar S, Erdem M. Activated carbons from waste biomass by sulfuric acid activation and their use on methylene blue adsorption. Bioresource Technology 2008; 99(14):6214-22.

Khuluk RH, Rahmat A, Buhani, Suharso. Removal of methylene blue by adsorption onto activated carbon from coconut shell (*Cocous nucifera* L.). Indonesian Journal of Science and Technology 2019;4(2):229-40.

Lesbani A, Asri F, Palapa NR, Taher T, Rachmat A. Efficient removal of methylene blue by adsorption using composite based Ca/Al layered double hydroxide-biochar. Global NEST Journal 2020;22(2):250-7.

Li J, Zhao P, Li T, Lei M, Yan W, Ge S. Pyrolysis behavior of hydrochar from hydrothermal carbonization of pinewood sawdust. Journal of Analytical and Applied Pyrolysis 2020c;146(12):Article No. 104771.

Li Y, Peng L, Li W. Adsorption behaviors on trace Pb^{2+} from water of biochar adsorbents from konjac starch. Adsorption Science and Technology 2020b;38(9-10):344-56.

Li Z, Sellaoui L, Gueddida S, Dotto GL, Ben Lamine A, Bonilla-Petriciolet A, et al. Adsorption of methylene blue on silica nanoparticles: Modelling analysis of the adsorption mechanism via a double layer model. Journal of Molecular Liquids 2020a;319:Article No. 114348.

Liao W, Wang H, Li HQ, Yang P. Fe(II) Removal from aqueous solution by layered double hydroxide/graphene composites: Adsorption coupled with surface oxidation. Environmental Engineering Science 2020;37(1):43-52.

Lu Y, Chen J, Zhao L, Zhou Z, Qiu C, Li Q. Adsorption of rhodamine b from aqueous solution by goat manure biochar: Kinetics, isotherms, and thermodynamic studies. Polish Journal of Environmental Studies 2020;29(4):2721-30.

Mahmuda KN, Wen TH, Zakaria ZA. Activated carbon and biochar from pineapple waste biomass for the removal ofmethylene blue. Environmental and Toxicology Management 2021;1(1):30-6.

Mantasha I, Saleh HAM, Qasem KMA, Shahid M, Mehtab M, Ahmad M. Efficient and selective adsorption and separation of methylene blue (MB) from mixture of dyes in aqueous environment employing a Cu(II) based metal organic framework. Inorganica Chimica Acta 2020;511:Article No. 119787.

Mishra S, Sahoo SS, Debnath AK, Muthe KP, Das N, Parhi P. Cobalt ferrite nanoparticles prepared by microwave hydrothermal synthesis and adsorption efficiency for organic dyes: Isotherms, thermodynamics and kinetic studies. Advanced Powder Technology 2020;31(11):4552-62.

Nakhli A, Bergaoui M, Toumi KH, Khalfaoui M, Benguerba Y, Balsamo M, et al. Molecular insights through computational modeling of methylene blue adsorption onto low-cost adsorbents derived from natural materials: A multi-model's approach. Computers and Chemical Engineering 2020; 140:Article No. 106965.

Normah N, Juleanti N, Siregar PMSBN, Wijaya A, Palapa NR, Taher T, et al. Size selectivity of anionic and cationic dyes using LDH modified adsorbent with low-cost rambutan peel to hydrochar. Bulletin of Chemical Reaction Engineering and Catalysis 2021a;16(4):869-80.

Normah, Palapa NR, Taher T, Mohadi R, Utami HP, Lesbani A. The ability of composite Ni/Al-carbon based material toward readsorption of iron(II) in aqueous solution. Science and Technology Indonesia 2021b;6(3):156-65.

Oliveira EIS, Santos JB, Gonçalves APB, Mattedi S, José NM. Characterization of the rambutan peel fiber (*Nephelium lappaceum*) as a lignocellulosic material for technological applications. Chemical Engineering Transactions 2016; 50:391-6.

Palapa NR, Taher T, Mohadi R, Rachmat A, Lesbani A. Preparation of copper aluminum-biochar composite as adsorbent of malachite green in aqueous solution. Research Square 2020a;524:1-24.

Palapa NR, Taher T, Rahayu BR, Mohadi R, Rachmat A, Lesbani A. CuAl LDH/Rice husk biochar composite for enhanced adsorptive removal of cationic dye from aqueous solution. Bulletin of Chemical Reaction Engineering and Catalysis 2020b;15(2):525-37.

Rafatullah M, Sulaiman O, Hashim R, Ahmad A. Adsorption of methylene blue on low-cost adsorbents: A review. Journal of Hazardous Materials 2010;177(1-3):70-80.

Rathee G, Awasthi A, Sood D, Tomar R, Tomar V, Chandra R. A new biocompatible ternary layered double hydroxide adsorbent for ultrafast removal of anionic organic dyes. Scientific Reports 2019;9(1):Article No. 16225.

Setiawan IKA, Napitupulu M, Walanda DK. Biocharcoal dari Kulit Rambutan (*Nephelium lappaceum* L.) sebagai Adsorben Zink dan Tembaga. Jurnal Akademika Kimia 2018; 7(4):Article No. 193.

Shin J, Kim K, Hong J. Zn-Al layered double hydroxide thin film. Coating 2020;10(669):1-7.

Stjepanović M, Velić N, Galić A, Kosović I, Jakovljević T, Habuda-Stanić M. From waste to biosorbent: Removal of congo red from water by waste wood biomass. Water 2021:13(3):Article No. 279.

Wang S, Gao B, Li Y, Zimmerman AR, Cao X. Sorption of arsenic onto Ni/Fe layered double hydroxide (LDH)-biochar composites. RSC Advances 2016;6:17792-9.

Wang W, Zhang N, Shi Z, Ye Z, Gao Q, Zhi M, et al. Preparation of Ni-Al layered double hydroxide hollow microspheres for supercapacitor electrode. Chemical Engineering Journal 2018;338:55-61.

Wang Z, Zhang L, Fang P, Wang L, Wang W. Study on simultaneous removal of dye and heavy metal Ions by NiAl-layered double hydroxide films. ACS Omega 2020; 5(34):21805-14.

Wijaya A, Siregar PNBSM, Priambodo A, Palapa NR, Taher T, Lesbani A. Innovative modified of Cu-Al/C (C=Biochar, Graphite) composites for removal of procion red from aqueous solution. Science Technology Indonesia 2021;6(4):228-34.

Wu J, Xia A, Chen C, Feng L, Su X, Wang X. Adsorption thermodynamics and dynamics of three typical dyes onto bio-adsorbent spent substrate of *Pleurotus eryngii*. International Journal of Environmental Research and Public Health 2019;16(5):Article No. 679.

Xu H, Zhang P, Zhou SY, Jia Q. Fullerene functionalized magnetic molecularly imprinted polymer: Synthesis, characterization and application for efficient adsorption of methylene blue. Chinese Journal of Analytical Chemistry 2020;48(9):e20107-e20113.

Xu H, Zhu S, Xia M, Wang F. Rapid and efficient removal of diclofenac sodium from aqueous solution via ternary core-shell CS@PANI@LDH composite: Experimental and adsorption mechanism study. Journal of Hazardous Materials 2021;402:Article No. 123815.

Yeow PK, Wong SW, Hadibarata T. Removal of azo and anthraquinone dye by plant biomass as adsorbent: A review. Biointerface Research in Applied Chemistry 2021;11(1): 8218-32.

Zhao J, Huang Q, Liu M, Dai Y, Chen J, Huang H, et al. Synthesis of functionalized MgAl-layered double hydroxides via modified mussel inspired chemistry and their application in organic dye adsorption. Journal of Colloid and Interface Science 2017;505:168-77.

Zhao Y, Zhan L, Xue Z, Yusef KK, Hu H, Wu M. Adsorption of Cu (II) and Cd (II) from wastewater by sodium alginate modified materials. Journal of Chemistry 2020;2020:Article No. 5496712.

Zubair M, Jarrah N, Ihsanullah KA, Manzar MS, Kazeem TS, Al-Harthi MA. Starch-NiFe-layered double hydroxide composites: Efficient removal of methyl orange from aqueous phase. Journal of Molecular Liquids 2018;249:254-64.

M2+(Ni, Cu, Zn)Al-LDH Composites with Hydrochar from Rambutan Peel and Study the Adsorption Efficiency for Organic Dyes.pdf

ORIGINALITY REPORT

13%
SIMILARITY INDEX

PRIMARY SOURCES

1	sciencetechindonesia.com Internet	245 words — 4%
2	dns2.asia.edu.tw Internet	106 words — 2%
3	pdfs.semanticscholar.org Internet	104 words — 2%
4	www.ecoeet.com Internet	88 words — 1%
5	doaj.org Internet	73 words — 1%
6	idoc.pub Internet	61 words — 1%
7	ir.jkuat.ac.ke Internet	44 words — 1%
8	ijoems.com Internet	43 words — 1%
9	www.jeeng.net Internet	35 words — 1%